

Folding Energetics in Thin-Film Diaphragms

Gustavo Gioia^a, Antonio DeSimone^b, Michael Ortiz^c, and Alberto M. Cuitiño^d

Urbana, April 30, 2000

^a Department of Theoretical & Applied Mechanics, University of Illinois, Urbana, IL 61801, USA.

^b Max Planck Institute for Mathematics in the Sciences, 04103 Leipzig, Germany.

^c Graduate Aeronautical Laboratories, California Institute of Technology, Pasadena, CA 91125, USA.

^d Department of Mechanical & Aerospace Engineering, Rutgers University, Piscataway, NJ 08854, USA.

We perform experiments on thin-film diaphragms to show that the folding patterns of anisotropically compressed diaphragms are strikingly different from those of isotropically compressed ones. We then use a simple von Kármán model to relate the overall features of these folding patterns to the underlying energetics. We show that the differences between the isotropic and anisotropic cases can be traced back to fundamental changes in the energy structure of the diaphragms. Finally, we point out that the energy structure of thin-film diaphragms is similar to that of many other systems in physics and engineering, into which our study may provide interesting insights.

Consider a film of thickness h bonded to the flat surface of a substrate except over a

domain Ω of characteristic size d , Fig. 1(a). The portion Ω of the film is a *diaphragm* [1]. If we apply a strain ϵ^* to the substrate, in the plane of the film, the diaphragm may deflect out of the substrate and fold [2]. We study the conditions which ϵ^* must fulfill for this to occur, and the nature of the resulting folding.

We prepared diaphragms by gluing paper sheets and polymeric films ($h \sim 0.01$ to 0.1 mm) onto substrates (thickness ~ 30 mm) of the shape shown in Fig. 1(a), made of a high-density styrofoam [3]. Then we compressed the substrates in two perpendicular directions, x_1 and x_2 , using screw-driven steel plates. When the applied strain components are equal to each other, $\epsilon_1^* = \epsilon_2^*$, the strain is *isotropic*; otherwise it is *anisotropic*. Figs. 1(b-c) show the folding of two equally shaped diaphragms subject to isotropic strains. The folding pattern is the same in both diaphragms; the number and spatial arrangement of the folds depend exclusively on the shape of Ω , being independent of d/h and of the strain. A completely different situation obtains when the strains are anisotropic. The folds are then perpendicular to the direction of ϵ_1^* (where $\epsilon_1^* > \epsilon_2^*$ by convention), regardless of the shape of Ω , Figs. 1(d-e). The number of folds depends on d/h , however, see Figs. 1(e-g); a comparison of Figs. 1(e) and (h) reveals that it depends also on the strain.

For the analysis of these results we follow [2] in *i*) modeling the film as a von Kármán plate, and *ii*) constraining the in-plane displacements of the diaphragm to remain null. As we shall show, this simple model allows for a straightforward energetic interpretation of the overall characteristics of folding patterns in thin-film diaphragms; the study of specific features of the folding, as well as of folding in structures other than diaphragms, may

require the consideration of the in-plane displacements [4]. For the proposed model the bending energy density at a point (x_1, x_2) of the diaphragm is

$$\varphi^b = \frac{Ch^2}{12} [(1 - \nu)(w_{,11}^2 + w_{,22}^2 + 2w_{,12}^2) + \nu(w_{,11} + w_{,22})^2], \quad (1)$$

and the membrane energy density is

$$\varphi^m = \frac{C}{2} \left[\frac{1}{4} (|\nabla w|^2 - 2(\epsilon_1^* + \nu\epsilon_2^*))^2 + (1 - \nu)w_{,2}^2(\epsilon_1^* - \epsilon_2^*) \right] + \varphi_{\min}^m, \quad (2)$$

where $C = Eh/(1 - \nu^2)$ is the membrane stiffness of the film; E is the Young modulus and ν the Poisson ratio of the film; w is the out-of-plane deflection of the diaphragm; $\nabla w = (w_{,1}, w_{,2})$ is the gradient of w ; $|\nabla w| = (w_{,1}^2 + w_{,2}^2)^{1/2}$ is the largest slope of the diaphragm at the given point; and we have defined $\varphi_{\min}^m = C(1 - \nu^2)(\epsilon_2^*)^2/2$. The total energy of the diaphragm is the sum of the bending and membrane energies, $\Phi = \Phi^m + \Phi^b$, where Φ^m and Φ^b are the integrals over Ω of φ^m and φ^b , respectively. We search a folding, described by $w(x_1, x_2)$, which minimizes $\Phi[w]$ subject to the conditions $w = 0$ and $w_{,n} = 0$ on the boundary, Fig. 1(a).

We start by noting that Φ^b and Φ^m are of order h^3 and h , respectively. Since we are interested in the thin-film limit, $h \rightarrow 0$, we expect Φ^m to admit one or more minimizers with the same overall structure as the minimizer of Φ . We know that in the minimizers of Φ^m the folds will not be rounded, but take the form of lines of slope discontinuity or *sharp folds*. (The reason is that Φ^m contains first derivatives of w only.) The bending energy will be confined to these sharp folds, in the form of an energy per unit length of sharp fold [5,6]. We plan to *i*) find the foldings which minimize Φ^m , and then *ii*) select

among them the one which contains the least sharp-fold energy; this one we shall call the *preferred folding* [2,7,8].

We try to minimize Φ^m by minimizing its integrand, φ^m , Eq. 2. For convenience we define a *compressive regime* $\epsilon_1^* + \nu\epsilon_2^* > 0$, and a *characteristic slope* $k = \sqrt{\epsilon_1^* + \nu\epsilon_2^*}$. We look for gradients $\nabla w = (w_{,1}, w_{,2})$ for which φ^m attains a minimum. When ϵ^* falls outside the compressive regime, a single minimum exists for $\nabla w = (0, 0)$, and the diaphragm remains flat. In the isotropic case, $\epsilon_1^* = \epsilon_2^*$, infinitely many minima of value φ_{\min}^m exist in the compressive regime; they occur for $|\nabla w| = k$, *i.e.* whenever the largest slope equals the characteristic slope. In the anisotropic case, two minima of value φ_{\min}^m exist in the compressive regime; they occur when $\nabla w = (\pm k, 0)$. Thus for a diaphragm in the compressive regime the minimum possible of the membrane energy is $\Phi_{\inf}^m = \varphi_{\min}^m A_\Omega$, where A_Ω is the area of the diaphragm. For convenience we shall work with $\tilde{\varphi}^m = \varphi^m - \varphi_{\min}^m$, which implies $\tilde{\Phi}^m = \Phi^m - \Phi_{\inf}^m$, and $\tilde{\Phi}_{\inf}^m = 0$.

We study the isotropic case first. Consider a 1D example in which we impose the constraint $w_{,2} = 0$. Then, the minima of $\tilde{\varphi}^m$ occur for $w_{,1} = \pm k$, and we can construct a minimizer of $\tilde{\Phi}^m$ by covering Ω with any set of *simple roofs* of slopes $\pm k$ (such as R_1 , R_2 and R_3 in Fig. 2(a)), and then choosing their upper envelope. Infinitely many such minimizers exist, all of which contain sharp folds, as expected. To minimize the energy associated with the sharp folds, we must minimize their number; this we effect by selecting the upper envelope of all the minimizers, Fig. 2(a). In 2D a preferred folding can be found analogously, as the upper envelope of all the possible cobertures of Ω with conical roofs of

slope k , Fig. 2(b) [2,9]. The preferred folding so selected does *i*) minimize Φ^m ; *ii*) depend exclusively on the shape of Ω ; and *iii*) match the experimental observations, as shown by a comparison of Fig. 2(c) with Figs. 1(b) and (c).

Now we turn to the anisotropic case. Consider first the infinite diaphragm of Fig. 3(a). For this diaphragm the preferred folding can be found as in the 1D isotropic case, in the form of a single simple roof of slopes $w_{,1} = \pm k$, Fig. 3(a). In the finite diaphragm of Fig. 3(b), on the other hand, a single simple roof violates the boundary conditions $w(x_2 = 0) = w(x_2 = 3/2) = 0$. To circumvent this problem we try the folding w_0 of Fig. 3(b). On the triangular regions of Fig. 3(b), which we call *closure domains*, $w_{,1} \neq \pm k$, and therefore $\tilde{\varphi}_\Delta^m > \tilde{\varphi}_{\min}^m$. It follows that w_0 is not a minimizer. In fact, calling $A_\Delta[w_0]$ the area of the closure domains, $\tilde{\Phi}^m[w_0] = \tilde{\varphi}_\Delta^m A_\Delta[w_0] > \tilde{\Phi}_{\inf}^m$. We can approach the minimum value $\tilde{\Phi}_{\inf}^m = 0$, however, by using foldings w_j with $j = 1, 2, \dots$, *e.g.* Fig. 3C, for which $A_\Delta[w_j] \rightarrow 0$ and therefore $\tilde{\Phi}^m[w_j] = \tilde{\varphi}_\Delta^m A_\Delta[w_j] \rightarrow 0$ as $j \rightarrow \infty$. Thus $\tilde{\Phi}^m$ can be made arbitrarily close to its minimum by allowing the diaphragm to become highly folded. The sequence w_j is said to be a *minimizing sequence*, and the associated foldings are called *microstructures* [10,11].

For arbitrarily shaped diaphragms, we can construct minimizing sequences in an analogous way, *e.g.* Fig. 3(d). All the microstructures in a minimizing sequence contain sharp folds and closure domains. As the microstructures become more folded, the sharp-fold energy increases, and the closure-domain energy decreases. In principle, we can identify a preferred microstructure for which the trade off between closure-domain energy and sharp-

fold energy is resolved in the least total energy. Thus bending checks the infinite folding implied by a minimizing sequence [10]. A straightforward dimensional analysis reveals that the number of folds N in the preferred microstructure scales with $\tilde{\varphi}_{\Delta}^m d/T$, where T is the energy per unit length of sharp fold. Setting $\epsilon_2^* = 0$ for the sake of simplicity, it is easy to conclude that $\tilde{\varphi}_{\Delta}^m \propto E(\epsilon_1^*)^2 h$; a more involved analysis leads to $T \propto E(\epsilon_1^*)^{3/2} h^2$ [12]. Therefore,

$$N \propto \frac{d}{h} (\epsilon_1^*)^{1/2}. \quad (3)$$

According to this expression, the number of folds for the diaphragms of Figs. 1(d-h) should be proportional to 32, 30, 16, 10 and 22, respectively. The observed numbers are 32, 28, 24, 12, and 22 (folds spanning the whole diaphragm). We conclude that the preferred microstructure of the minimizing sequence does *i*) fail to minimize Φ^m ; and *ii*) contain, in accord with the experimental evidence, folds which are perpendicular to the direction of ϵ_1^* , regardless of the shape of Ω , in a number which scales with d/h and ϵ^* in the form of Eq. (3).

To sum up, the folding of compressed diaphragms can be interpreted in terms of two operations: fold to release membrane energy, and then allow bending to select one among many possible foldings. In the isotropic case, infinitely many foldings exist which can accommodate the boundary conditions and simultaneously minimize Φ^m . Out of these foldings bending selects a preferred one. In the anisotropic case, no folding exists which can accommodate the boundary conditions and simultaneously minimize Φ^m . It is possible, however, to construct sequences of increasingly fine foldings, or microstructures, whose

associated membrane energies converge to the minimum value of Φ^m . Out of these foldings bending selects a preferred one.

The occurrence of microstructures in compressed diaphragms discloses a mathematical similarity with many problems including solidification [13], solid-state phase transformation [14], epitaxial thin-film growth [15], crystal plasticity [16], ferromagnetism [17], *et cetera*, where microstructures have been documented in the form of eutectic structures, twinning, film roughening, dislocation cells, and magnetic domain structures, respectively. Other such problems are coagulation [18], stretching of solid foams [19], and self-assembly of polymer layers on patterned substrates [20]. Because experiments can be easily performed on compressed diaphragms, and a simple model appears to explain their behavior well, the study of diaphragms may prove useful to gain insights into many other systems. For example, a 90 degree rotation of the gradients in Figs. 3(b-d) leads to closed-flux vector fields such as they obtain in ferromagnets, where magnetic poles are energetically penalized [17]. In this analogy, sharp folds model ferromagnetic domain walls, and strain anisotropy models crystalline anisotropy. A comparison of the fold branching observable close to diaphragm boundaries, *e.g.* Fig. 1(g), with the analogous phenomenon of domain branching in the vicinity of free surfaces in ferromagnets [21] would enhance our understanding of the underlying energetics. Supported by a grant from the Mechanics and Structures of Materials Program, NSF, Dr. K. P. Chong, Program Director.

References and notes

1. Thin-film diaphragms have elicited much interest in recent years because of their applications in micro electro-mechanical systems; see almost any chapter in M. Madou, *Fundamentals of Microfabrication* (CRC Press, Boca Raton, Florida, 1997).
2. G. Gioia, G., and M. Ortiz, *Adv. Appl. Mech.* **33**, 119 (1997).
3. A relatively high density ($\sim 40 \text{ kg/m}^3$) is required for the foam to deform homogeneously. In fact, low-density solid foams display deformation patterns which are analogous to the folding patterns of anisotropically compressed diaphragms; see also [19].
4. A. Lobkovsky, S. Gentges, H. Li, D. Morse, and T. Witten, *Science* **270**, 1482 (1995); E. Cerda, S. Chaieb, F. Melo, and L. Mahadevan, *Nature* **401**, 46 (1999).
5. L. Modica, *Arch. Rat. Mech. Anal.* **98**, 123 (1987).
6. R. V. Kohn, and S. Müller, *Comm. Pure Appl. Math.*, **47**, 405 (1994).
7. E. de Giorgi, *Rendiconti di Matematica* **8**, 277 (1975).
8. P. Sternberg, *Arch. Rat. Mech. Anal.* **101**, 209 (1988).
9. W. Jin, *Singular Perturbation and the Energy of Folds*, PhD Thesis, Courant Institute of Mathematical Sciences, New York University (1997).
10. J. M. Ball, and R. D. James, *Arch. Ration. Mech. Anal.* **100**, 13 (1987).
11. R. V. Kohn, *Continuum Mech. Thermodyn.* **3**, 193 (1991).

12. G. Gioia, A. DeSimone, and A. M. Cuitiño (to be published).
13. J. W. Cahn, *Acta Metall.* **9**, 795 (1961).
14. A. G. Kachaturyan, *Theory of Structural Transformations in Solids*. (J. Willey & Sons, New York, 1983).
15. C. Orme, and B. G. Orr, *Surf. Rev. Lett.* **4**, 71 (1997).
16. M. Ortiz, and E. A. Repetto, *J. Mech. Phys. Solids* **47**, 397 (1999).
17. A. DeSimone, *Arch. Ration. Mech. Anal.* **125**, 99 (1993).
18. J. Carr and R. Pego, *Proc. Roy. Soc. London*, **A436**, 569 (1992).
19. Y. Wang, G. Gioia, A. M. and Cuitiño (to be published).
20. M. Böltau, S. Walheim, J. Mlynek, G. Krausch, and U. Steiner, *Nature* **391**, 877 (1998).
21. R. V. Kohn and S. Müller, *Phil. Mag.* **A66**, 697 (1992).
22. A. S. Argon, V. Gupta, H. S. Landis, and J. A. Cornie, *J. Mater. Sci.* **24**, 1207 (1989).

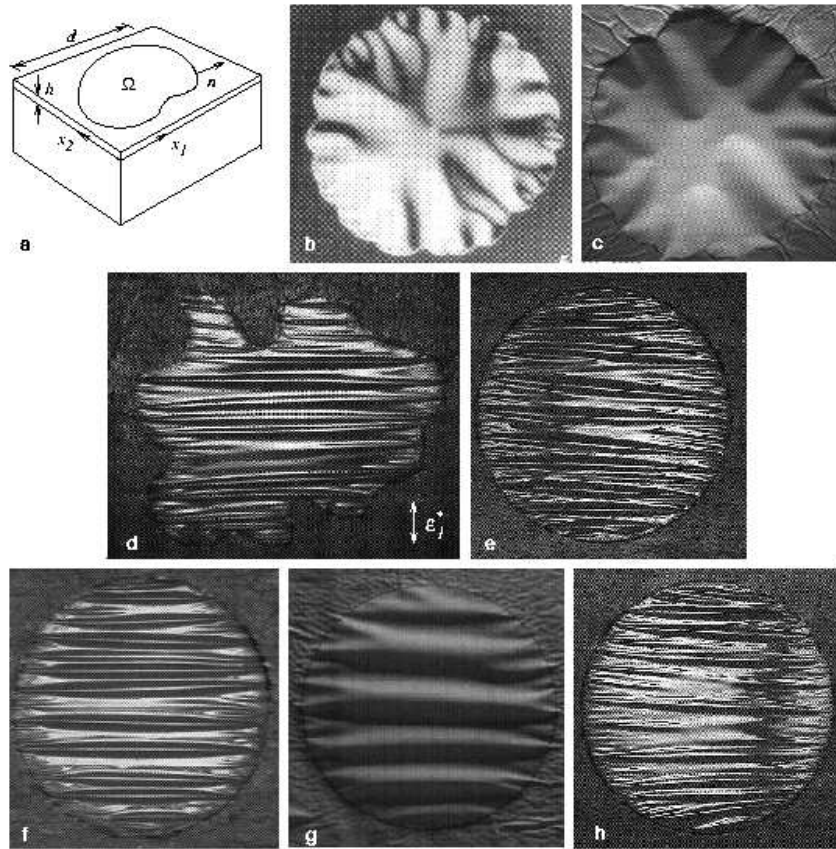


Figure 1: **a**, Thin film/substrate system, diaphragm, and notation. Top view of folded diaphragms: **b**, SiC film, $\epsilon_1^* = \epsilon_2^* = 0.011$, $d/h = 140$ [22]. **c**, Paper film, $\epsilon_1^* = \epsilon_2^* = 0.040$, $d/h = 950$. The following are polymeric films (except when noted) with $\epsilon_2^* = 0$: **d**, $\epsilon_1^* = 0.038$, $d/h = 5600$. **e**, $\epsilon_1^* = 0.035$, $d/h = 5600$. **f**, $\epsilon_1^* = 0.035$, $d/h = 2840$. **g**, Paper film, $\epsilon_1^* = 0.040$ $d/h = 1800$. **h**, $\epsilon_1^* = 0.019$, $d/h = 10600$.

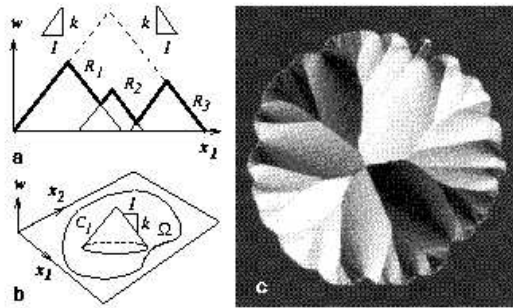


Figure 2: Analysis of the isotropic case. **a**, Side view of a 1D, constrained diaphragm covered with a set of three simple roofs of slopes $\pm k$, the associated minimizer (bold lines), and the preferred folding (dashed lines). **b**, A 2D diaphragm and an example of conical roof of slope k , denoted C_1 . **c** Preferred folding for the diaphragm shape of Figs. 1(b) and (c).

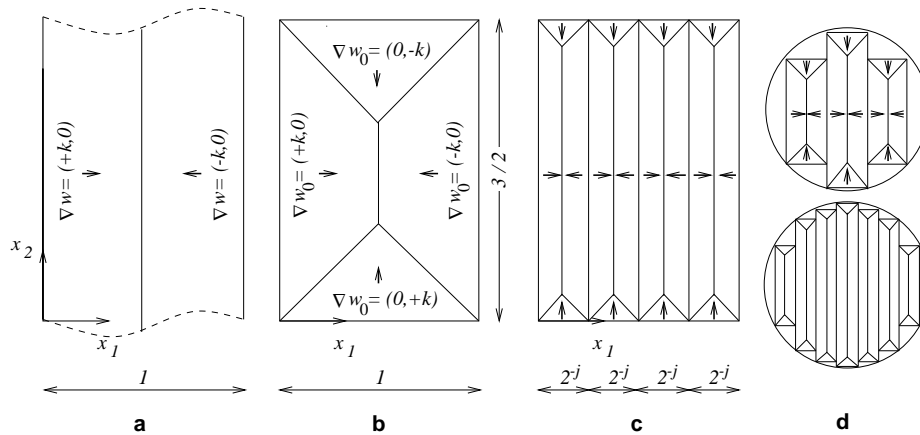


Figure 3: Analysis of the anisotropic case. **a**, Top view of a semi-infinite diaphragm with preferred folding. **b**, Rectangular diaphragm with folding w_0 . **c**, Idem with w_2 (i.e. the microstructure $j = 2$ of the minimizing sequence w_j). **d**, Two terms of a minimizing sequence for a circular diaphragm.